Hindawi Publishing Corporation
International Journal of Photoenergy
Volume 2016, Article ID 3675036, 7 pages
http://dx.doi.org/10.1155/2016/3675036

Research Article

Stable Inverted Low-Bandgap Polymer Solar Cells with Aqueous Solution Processed Low-Temperature ZnO Buffer Layers

Chunfu Zhang,[1] Shangzheng Pang,[1] Ting Heng,[1] Hailong You,[1] Genquan Han,[1] Gang Lu,[2] Fengqin He,[2] Qubo Jiang,[3] and Jincheng Zhang[1]

[1]*State Key Discipline Laboratory of Wide Band Gap Semiconductor Technology, School of Microelectronics, Xidian University, 2 South Taibai Road, Xi'an 710071, China*
[2]*Huanghe Hydropower Solar Industry Technology Co., Ltd., 369 South Yanta Road, Xi'an 710061, China*
[3]*Guilin University of Electronic Technology, No. 1 Jinji Road, Guilin 541004, China*

Correspondence should be addressed to Chunfu Zhang; cfzhang@xidian.edu.cn and Hailong You; hlyou@mail.xidian.edu.cn

Received 6 May 2016; Revised 21 August 2016; Accepted 24 August 2016

Academic Editor: Hongxia Wang

Efficient inverted low-bandgap polymer solar cells with an aqueous solution processed low-temperature ZnO buffer layer have been investigated. The low-bandgap material PTB-7 is employed so that more solar light can be efficiently harvested, and the aqueous solution processed ZnO electron transport buffer layer is prepared at 150°C so that it can be compatible with the roll-to-roll process. Power conversion efficiency (PCE) of the inverted device reaches 7.12%, which is near the control conventional device. More importantly, the inverted device shows a better stability, keeping more than 90% of its original PCE after being stored for 625 hours, while PCE of the conventional device is only 75% of what it was. In addition, it is found that the ZnO thin film annealed in N_2 can obviously increase PCE of the inverted device further to 7.26%.

1. Introduction

As an efficient way to utilize the solar energy, solar cells attract great research interests all over the world. In various solar cells, due to the potential of low cost, large area fabrication process, light weight physical feature, and compatibility with roll-to-roll fabrication, polymer solar cells (PSCs) are of tremendous interest and the performance was steadily improving [1–5]. Power conversion efficiency (PCE) above 10% has been reported recently based on the widely used bulk heterojunction (BHJ) of polymer-fullerene blend [5–9]. Usually, in one efficient solar cell, the absorption of active layer should match well with the solar spectrum to generate as many excitons as possible. Since the absorption ability of fullerene is weak, polymer has to undertake the main responsibility for absorbing solar light. It is well known that about 70% of the solar energy concentrates in the range of 380 nm to 900 nm in the solar spectrum, so the ideal polymeric material should have strong absorption in this range. In other words, the bandgap of polymeric material should be less than 1.6 eV, and the narrower the bandgap is, the wider the absorption range it will own, which will lead to higher short current density (J_{SC}). Materials scientists and chemists are further studying the polymeric material and making full use of its advantage of being tailorable to obtain material with narrower bandgap. In recent years, poly({4,8-bis[(2-ethylhexyl)oxy]benzo[1,2-b:4,5-b′]dithiophene-2,6-diyl}{3-fluoro-2-[(2-ethylhexy)carbonyl]thieno[3,4-b]thiophenediyl}) (PTB-7), one low-bandgap material, has been used in PSCs and achieved great success.

Besides the pursuit of higher PCE, people are trying new device structure and adopting different material to modify electrodes in order to get more stable PSCs. It is well known that there are two structures mainly used in PSCs, inverted and conventional structure, according to the sequence of electrodes. In most conventional structures, poly(3,4-ethylenedioxythiophene):poly(styrene sulfonic acid) (PEDOT:PSS) is usually adopted as the hole transport layer (HTL) and a low-work-function metal (Ca or Al) as the electron transport layer (ETL). PEDOT:PSS is a doping conductive polymer with good stability of photoelectric and high light transmittance. However, acid PEDOT:PSS

may corrode the ITO electrode, and PSS is likely to react with the conjugated polymer in the active layer which will directly affect the stability of the device [3, 10–15]. Besides, PEDOT:PSS may form discontinuous surface morphology and electronic structure. As an active metal, Ca or Al is easily affected by trace amounts of water and oxygen in glove box and is likely to diffuse into the active layer and then affect PCE and stability of the devices [16, 17]. Compared with the conventional structure, inverted PSCs, which are realized by reversing the electrode polarity of the devices, have been considered as an advantageous approach to improving the cell stability and roll-to-roll fabrication process [10–18]. In inverted PSCs, the active layer is usually sandwiched by two metal oxide transport layers and a high-work-function metal (Au, Ag, and Cu) acts as the top anode, so the commonly used hole transport layer PEDOT:PSS and low-work-function metal top cathode in conventional structure can be both avoided, all ensuring good stability.

In inverted PSCs, metal oxides such as zinc oxide (ZnO), titanium oxide (TiO_x), and aluminium oxide (Al_2O_3) have been widely introduced as ETL to form an ohmic contact to decrease or eliminate the electron-extraction barrier between ITO cathode and active layer [19–24]. In particular, ZnO, which is II–VI compound semiconductor with the six-party lead-zinc mine structure and with bandgap width of around 3.4 eV, has been considered as a good candidate because of its beneficial properties such as high electron mobility and high transparency in visible and near infrared region [10–18]. Various methods including chemical vapor deposition, laser ablation, magnetron sputtering, electrochemical deposition, and solution method can be used to prepare ZnO. Among them, the solution processed method is more desirable, since it is time-saving, low-cost, simple, and compatible with printing techniques [3, 14, 23]. Several solution processed ZnO fabrication techniques have been studied, such as sol-gel, nanocrystalline ZnO particle (Nc-ZnO), and aqueous solution route [17, 22, 25]. However, because of the high-temperature process of sol-gel ZnO (usually $\geq 300^{\circ}$C) and environmentally sensitive electrical performance of Nc-ZnO, the aqueous solution of ammine-zinc complex has been reported to be a promising technique which could avoid these problems to afford low-temperature conversion to dense ZnO thin films [3, 15, 26–28].

In this paper, we employed the aqueous solution processed ZnO layer as ETL in inverted PSCs based on PTB-7:PC_{71}BM blends. Here, the low-bandgap material PTB-7 is used so that more solar light can be harvested by the device. And the ZnO ETL is prepared in a low-temperature process so that it can be compatible with the roll-to-roll process. The inverted device shows an improved stability. Research suggests that the ZnO annealing condition can affect the device performance. By optimizing these factors, the fabricated inverted PSCs show promising performance.

2. Experimental

The aqueous precursor solution used for ZnO buffer layer is first prepared [3, 14]. The ZnO powder (99.9%, particle size < 5 μm, Sigma-Aldrich) was dissolved in ammonia (25%, Tianjin Chemical Reagent Co.) to form 0.1 M ($Zn(NH_3)_4^{2+}$) solution; then the solution was refrigerated for more than 12 h before use. PTB-7 and [6,6]-phenyl C61 butyric acid methyl ester (PC_{71}BM) were purchased from 1-Material Inc. and Nano-C Inc., respectively. PTB-7 and PC_{71}BM were dissolved in chlorobenzene/1,8-diiodoctane (97 : 3 vol%) mixed solvent with the concentration of 25 mg/mL and 1 : 1.5 weight ratio. The solution of PTB-7:PC_{71}BM was stirred for 12 h before use. ITO coated glass substrates have a sheet resistance of about 10 Ω/sq and average transmission over 80% in the visible light region. The chlorobenzene and MoO_3 were provided by Aldrich Inc. All the materials were used without any further purification.

Conventional and inverted PSCs based on PTB-7:PC_{71}BM have been prepared in this work. As shown in Figure 1(a), the conventional PSC has the configuration of glass/ITO/PEDOT:PSS/PTB-7:PC_{71}BM/Ca/Ag and the inverted PSC has the configuration of glass/ITO/ZnO/PTB-7:PC_{71}BM/MoO_3/Ag. All the devices were fabricated on patterned ITO-coated glass substrates. ITO-coated glass substrates were cleaned sequentially with detergent (Decon 90, UK), deionized water, acetone, and ethanol in an ultrasonic bath for about 15 min and were blown dry with a nitrogen gun before use. For the conventional device, a layer of PEDOT:PSS was spin-coated on ITO at 3000 rpm for 40 s, following the oxygen plasma treatment of 10 min. Substrates were subsequently annealed at 150°C for 30 min in air and then transferred to the glove box. The PTB-7:PC_{71}BM film was spin-coated onto the PEDOT:PSS layer in glove box at 1200 rpm. The Ca/Ag cathode was finally thermally evaporated to define an active area of 12.5 mm^2. For the inverted device, ZnO aqueous solution was spin-coated onto cleaned ITO glass substrates at 3000 rpm for 40 s, followed by annealing in the oven under ambient condition or in N_2 at 150°C for 30 min. The PTB-7:PC_{71}BM film was prepared in the previous case. Finally, the MoO_3/Ag anode was thermally evaporated to define an active area of 12.5 mm^2.

A Keithley 2400 source measure unit and a Xenon lamp (XEC-300M2, SANEI ELECTRIC) with an AM 1.5G filter were utilized to measure the current density-voltage (J-V) characteristics of all the devices in air. The light intensity was adjusted to 100 mW/cm^2 by a standard solar cell calibrated by the National Renewable Energy Laboratory (NREL). Tapping mode AFM tests were performed to test the thin films morphology by an Agilent 5500 scanning probe system. The transmittance spectra were determined by UV-VIS spectrophotometer (Lanbda 950). The photoluminescence (PL) spectrum test was also performed to analyze the ZnO thin film using the 325 nm line of a He-Cd laser.

3. Results and Discussion

The corresponding energy band diagram of the inverted PSC is illustrated in Figure 1(b). ZnO has the conduction band energy of around −4.3 eV and the valance band energy of around −7.5 eV, which suggests that electrons from PC_{71}BM can be transported into ZnO, while holes from PTB-7 can

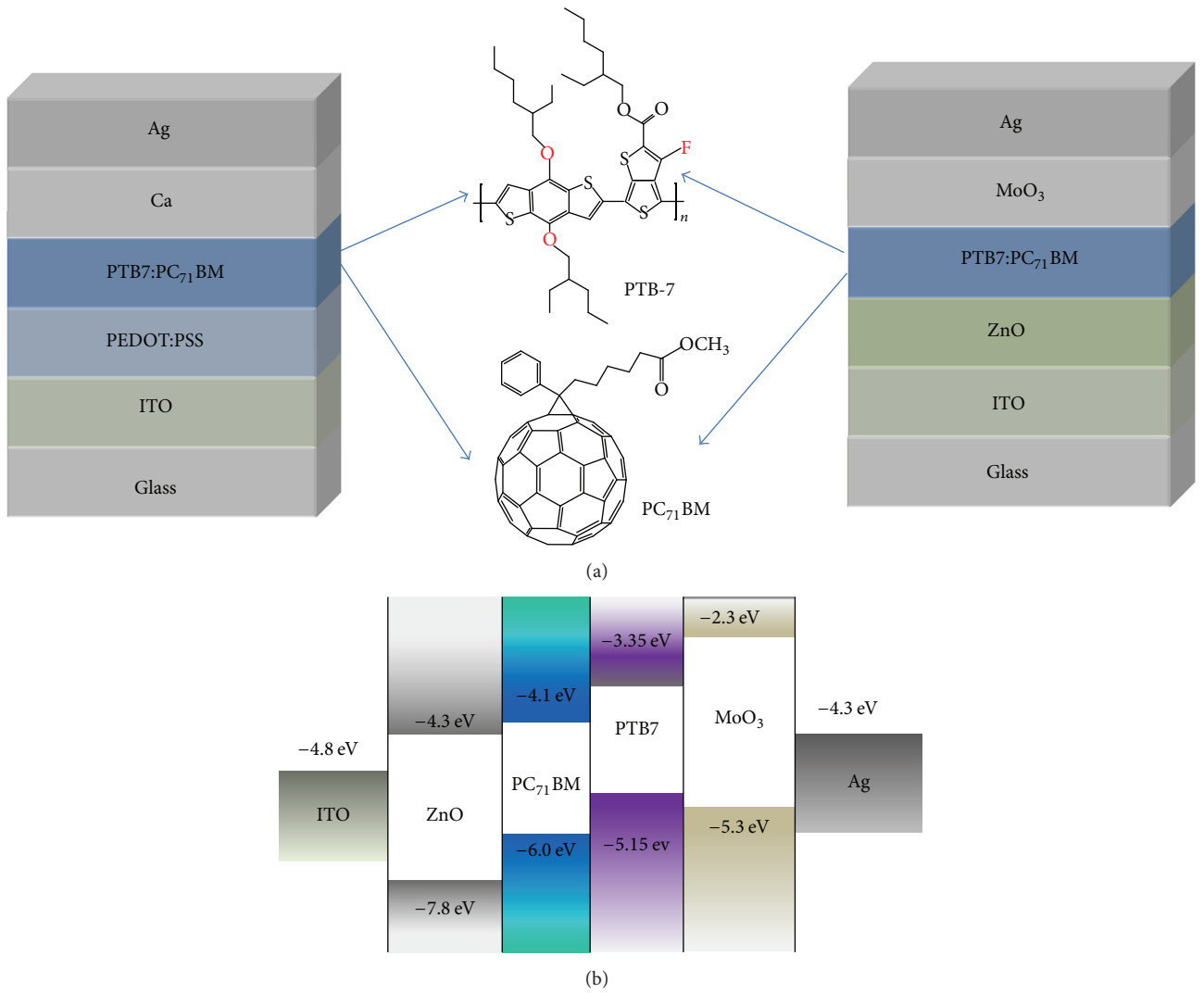

FIGURE 1: (a) Schematic device structures of conventional and inverted PSCs. (b) Energy level alignment of the components in the inverted PSC with ZnO as the electron transport layer.

be blocked. In other words, this ZnO acts as an electron-extraction layer and a hole blocking layer. Using ZnO to modify the ITO polarity has been proved to be a very efficient way to realize the inverted PSCs. At the same time, MoO_3 plays the role of electron blocking layer and it can effectively promote holes to transport into the anode.

Figure 2 shows the obtained light J-V curves of conventional and inverted PSCs under AM 1.5G illumination with 100 mW/cm^2 intensity and the corresponding device performances are also shown in Table 1. PSC with conventional structure prepared in this work has PCE of 8.39%, open-circuit voltage (V_{OC}) of 0.74 V, J_{SC} of 16.22 mA/cm^2, and fill factor (FF) of 69.61%. This is among the most efficient PSCs based on the PTB-7:$PC_{71}BM$ material system. For the inverted device with ZnO annealed under ambient condition, PCE achieves 7.12% with V_{OC} of 0.72 V, J_{SC} of 12.87 mA/cm^2, and FF of 69.85%. By comparing the inverted device with the conventional device, it is shown that J_{SC} of the inverted device is slightly lower than that of the conventional device, but for V_{OC} and FF there are no obvious differences. This shows that the ZnO layer has effectively changed the polarity of ITO electrode and acts as ETL.

The J-V characteristics of PSCs can be approximately described by the Shockley equation as

$$J = J_0 \left(\exp\left(\frac{q(V - R_s J)}{n k_B T} \right) - 1 \right) + \frac{V - R_s J}{R_{sh}} - J_{ph}, \quad (1)$$

where J_0 is the saturation current, J_{ph} the photocurrent, R_s the series resistance, R_{sh} the shunt resistance, n the ideality factor, q the electron charge, k_B the Boltzmann constant, and T the temperature, respectively. By using (1) with the proposed explicit analytic expression method [29], the experimental data can be well rebuilt as shown in Figure 2. The extracted photovoltaic parameters are also displayed in Table 1. The conventional device has a low series resistance and the inverted device has a relative high series resistance. Series resistance is affected by the morphology of the active layer

Table 1: Photovoltaic performance parameters for conventional and inverted PSCs with ZnO as ETL under the simulated AM 1.5G illumination of 100 mW/cm^2 fresh or stored after 625 hours.

Devices	V_{OC} (V)	J_{SC} (mA/cm^2)	FF (%)	PCE (%)	J_{ph} (mA/cm^2)	J_0 (mA/cm^2)	n	R_s Ωcm^2
Conventional	0.74	16.22	69.61	8.39	16.26	$3.31E-06$	1.87	1.7
Inverted (annealed in air)	0.74	13.92	69.12	7.12	13.95	$1.58E-05$	2.1	2.3
Inverted (annealed in nitrogen)	0.73	14.07	70.79	7.26	14.1	$1.60E-06$	1.77	2.7
Conventional (625 hours later)	0.75	12.74	65.26	6.26	12.82	$8.78E-07$	1.78	2
Inverted (annealed in air (625 hours later))	0.70	12.56	68.25	5.99	12.58	$1.59E-05$	2.00	1.4

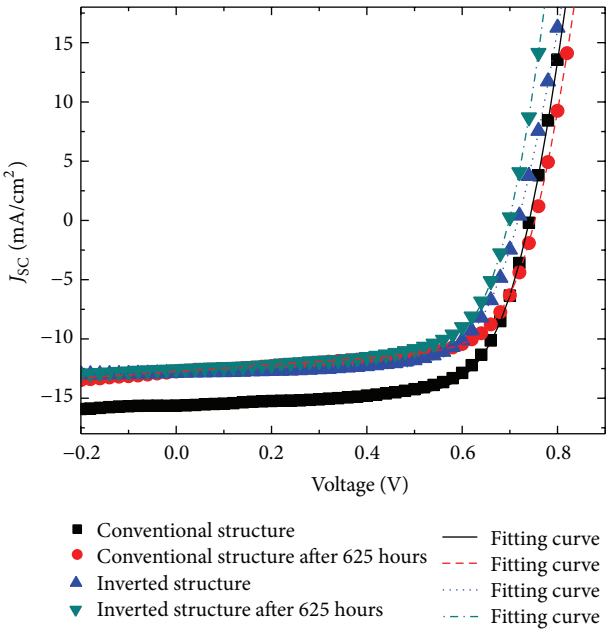

Figure 2: Measured (symbol) and calculated (line) J-V characteristics for conventional and inverted PSCs with ZnO as ETL under the simulated AM 1.5G illumination of 100 mW/cm^2 fresh or stored after 625 hours.

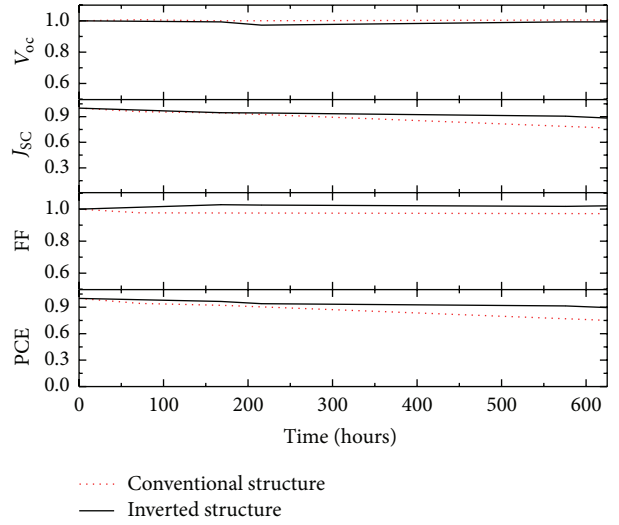

Figure 3: Normalized photovoltaic parameters of conventional and inverted PSCs as a function of storage time. The values are averages of five devices.

and the carrier transport layer. The main difference between the two structures is the carrier transport layer. The relative high series resistance means that the conductance of the used ZnO layer is relatively low. This can be improved by doping the ZnO layer, which will be our future work.

Besides PCE, the stability of solar cells is another important factor for the practical application. To compare the device stability between the two different structures, the unencapsulated PSCs were tested for 625 hours. Figure 3 shows the average performance parameters varying with the time for 5 devices and the typical J-V curves of PSCs after being tested for 625 hours are also shown in Figure 2. It is found that the conventional device has obvious degradation; however, the change of the J-V curve of inverted device is not evident. As shown in Figure 3, average PCE of inverted device still keeps 90% of its initial value after 625 hours, while the conventional device only keeps 75% of its original value. In all the parameters, V_{OC} and FF change slightly with the time

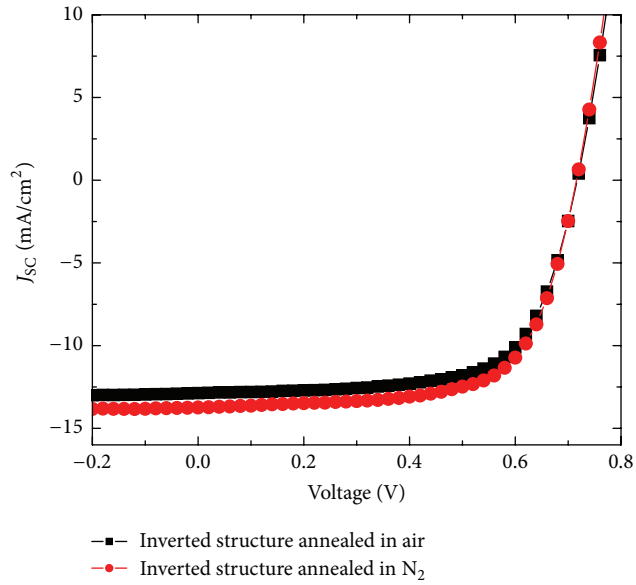

Figure 4: J-V characteristics for inverted OSCs with the ZnO buffer layer annealed in N_2 or air under the simulated AM 1.5G illumination of 100 mW/cm^2.

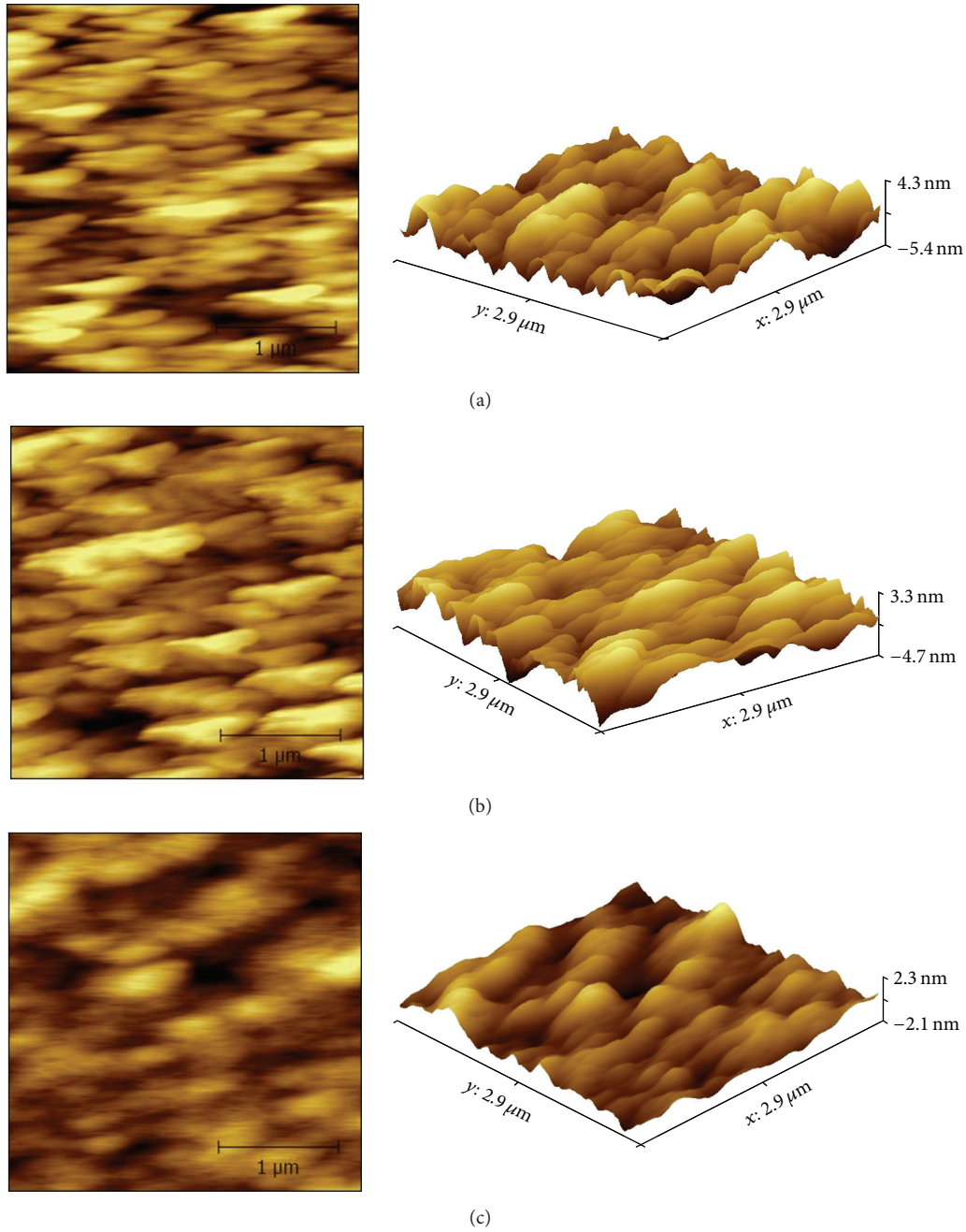

Figure 5: Surface morphologies of (a) ITO/PEDOT:PSS, (b) ITO/ZnO (annealed in air), and (c) ITO/ZnO (annealed in N_2).

going by. The decline of PCE is mainly due to the decrease of J_{SC}. However, J_{SC} change of the inverted device is obviously smaller than that of the conventional device and this makes the overall PCE of the inverted device change slightly. The improved stability in inverted structure has been reported in many reports [13, 15, 25] and our results confirm again that the inverted structure can greatly improve the device stability due to its obvious advantages as stated in Introduction.

In order to achieve a better ZnO layer, thermal annealing is one essential process. Adequate thermal annealing makes zinc oxide precursor form ZnO more thoroughly and evenly. At the same time, adequate thermal annealing also removes the solvent in the film. By a simple annealing process, a better morphology and crystallization of ZnO can be got. Our previous work has shown that an annealing temperature lower than 150°C is enough to achieve a good ZnO interlayer used in PSCs [14]. Here, annealing atmosphere is investigated further. It is found that solar cells with ZnO layer annealing in N_2 have better performance. The corresponding V_{OC} reaches 0.73 V, J_{SC} reaches 14.07 mA/cm^2, FF reaches 70.79%, and PCE reaches 7.26%. This means annealing in different atmosphere indeed causes different effects on performance

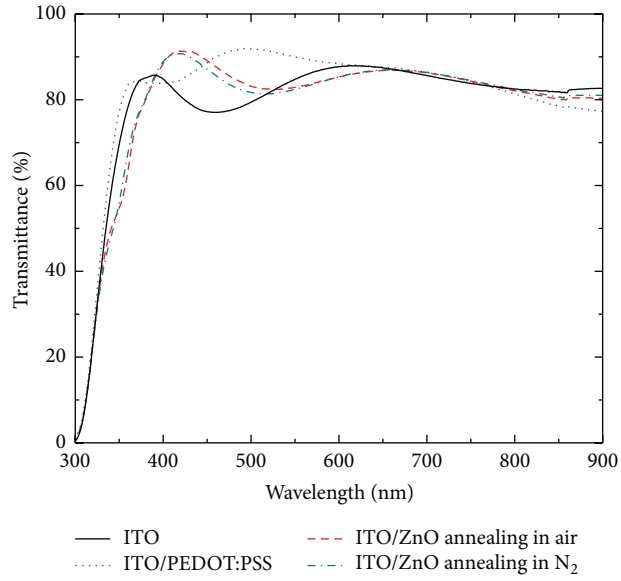

Figure 6: Wavelength-dependent transmittance spectra of ITO, ITO/ZnO annealed in air, ITO/ZnO annealed in N_2, and ITO/PEDOT:PSS.

of solar cells. Figure 4 shows the J-V curves of devices annealed under different conditions, and Table 1 shows their corresponding performance parameters. J_{SC} and FF of the inverted device annealed in N_2 are higher than those annealed in air. Annealing in N_2 may improve the quality of ZnO thin film, so the morphology of active layer and interface between ZnO layer and active layer are improved, which is beneficial for the transmission and collection of carriers.

AFM was adopted to characterize the morphology of ITO/PEDOT:PSS, ITO/ZnO (annealed in air), and ITO/ZnO (annealed in N_2). Figure 5 shows the results. It is found that ZnO annealed in air has the largest RMS of 1.66 nm, while the RMS of ZnO annealed in N_2 is only about 1.30 nm. The morphology of ITO/PEDOT:PSS was measured at the same time and its RMS is the lowest, just 0.64 nm. The better performance of the conventional device means that lower RMS or smooth and homogeneous PEDOT:PSS thin film is vital for OSCs. When ZnO is annealed in N_2, the RMS is lower than that annealed in air. This is one possible reason for the better performance of the device with ZnO annealed in N_2. The recent work has also shown that ZnO annealed in N_2 has higher carrier mobility than that annealed in air [30], and this is another reason for the better device performance.

UV-VIS spectrophotometer was adopted to measure the transmission spectrum of ZnO thin films annealed in different atmospheres as shown in Figure 6. It is found that ITO/PEDOT:PSS has better transmittance between 450 nm and 650 nm. It is in the absorption region of PTB-7:PC_{71}BM material system, and this may be one reason why the conventional device has a larger J_{SC}. However, the difference between the ITO/ZnO annealed in N_2 and that annealed in air is very small. Thus, it can be derived that the optical characteristics are not the main reason causing different performance for the device with ZnO annealed in N_2 and air.

4. Conclusion

Conventional and inverted PSCs based on PTB-7:PC_{71}BM were fabricated in this work. The low-bandgap material PTB-7 is employed so that more solar light can be harvested by the device. And ZnO ETL is prepared in a low-temperature process so that it can be compatible with the roll-to-roll process. PCE of the conventional device of more than 8% is achieved, and PCE of the inverted device also reaches 7.12%. The inverted device shows a better stability, keeping more than 90% of its original PCE after being stored after 625 hours, while PCE of the conventional device is only 75% of what it was. In addition, it is shown that the ZnO thin film annealed in N_2 can obviously increase PCE of the inverted device further to 7.26%.

Competing Interests

The authors declare that they have no competing financial interests and the mentioned received funding in Acknowledgments did not lead to any conflict of interests regarding the publication of this manuscript.

Acknowledgments

This study was partly financially supported by National Natural Science Foundation of China (61334002 and 61106063) and the Fundamental Research Funds for the Central Universities (JB141106).

References

[1] G. Yu, J. Gao, J. C. Hummelen, F. Wudl, and A. J. Heeger, "Polymer photovoltaic cells: enhanced efficiencies via a network of internal donor-acceptor heterojunctions," *Science*, vol. 270, no. 5243, pp. 1789–1791, 1995.

[2] H.-Y. Chen, J. Hou, S. Zhang et al., "Polymer solar cells with enhanced open-circuit voltage and efficiency," *Nature Photonics*, vol. 3, no. 11, pp. 649–653, 2009.

[3] W. Wei, C. Zhang, D. Chen et al., "Efficient "light-soaking"-free inverted organic solar cells with aqueous solution processed low-temperature ZnO electron extraction layers," *ACS Applied Materials and Interfaces*, vol. 5, no. 24, pp. 13318–13324, 2013.

[4] B. R. Lee, S. Lee, J. H. Park et al., "Amine-based interfacial molecules for inverted polymer-based optoelectronic devices," *Advanced Materials*, vol. 27, no. 23, pp. 3553–3559, 2015.

[5] V. Vohra, K. Kawashima, T. Kakara et al., "Efficient inverted polymer solar cells employing favourable molecular orientation," *Nature Photonics*, vol. 9, no. 6, pp. 403–408, 2015.

[6] B. Kan, Q. Zhang, M. Li et al., "Solution-processed organic solar cells based on dialkylthiol-substituted benzodithiophene unit with efficiency near 10%," *Journal of the American Chemical Society*, vol. 136, no. 44, pp. 15529–15532, 2014.

[7] J. Huang, C.-Z. Li, C.-C. Chueh, S.-Q. Liu, J.-S. Yu, and A. K.-Y. Jen, "10.4% Power conversion efficiency of ITO-free organic photovoltaics through enhanced light trapping configuration," *Advanced Energy Materials*, vol. 5, no. 15, Article ID 1500406, 2015.

[8] T. L. Nguyen, H. Choi, S.-J. Ko et al., "Semi-crystalline photovoltaic polymers with efficiency exceeding 9% in a ~300 nm

thick conventional single-cell device," *Energy and Environmental Science*, vol. 7, no. 9, pp. 3040–3051, 2014.

[9] Z. He, C. Zhong, S. Su, M. Xu, H. Wu, and Y. Cao, "Enhanced power-conversion efficiency in polymer solar cells using an inverted device structure," *Nature Photonics*, vol. 6, no. 9, pp. 591–595, 2012.

[10] M. Jørgensen, K. Norrman, S. A. Gevorgyan, T. Tromholt, B. Andreasen, and F. C. Krebs, "Stability of polymer solar cells," *Advanced Materials*, vol. 24, no. 5, pp. 580–612, 2012.

[11] J. Min, Y. N. Luponosov, Z.-G. Zhang et al., "Interface design to improve the performance and stability of solution-processed small-molecule conventional solar cells," *Advanced Energy Materials*, vol. 4, no. 16, Article ID 1400816, 2014.

[12] S. Savagatrup, A. D. Printz, T. F. O'Connor et al., "Mechanical degradation and stability of organic solar cells: molecular and microstructural determinants," *Energy and Environmental Science*, vol. 8, no. 1, pp. 55–80, 2015.

[13] O. Pachoumi, C. Li, Y. Vaynzof, K. K. Banger, and H. Sirringhaus, "Improved performance and stability of inverted organic solar cells with sol-gel processed, amorphous mixed metal oxide electron extraction layers comprising alkaline earth metals," *Advanced Energy Materials*, vol. 3, no. 11, pp. 1428–1436, 2013.

[14] D. Chen, C. Zhang, T. Heng et al., "Efficient inverted polymer solar cells using low-temperature zinc oxide interlayer processed from aqueous solution," *Japanese Journal of Applied Physics*, vol. 54, no. 4, Article ID 42301, 2015.

[15] D. Chen, C. Zhang, W. Wei et al., "Stability of inverted organic solar cells with low-temperature ZnO buffer layer processed from aqueous solution," *Physica Status Solidi (A)*, vol. 212, no. 10, pp. 2262–2270, 2015.

[16] J.-C. Wang, W.-T. Weng, M.-Y. Tsai et al., "Highly efficient flexible inverted organic solar cells using atomic layer deposited ZnO as electron selective layer," *Journal of Materials Chemistry*, vol. 20, no. 5, pp. 862–866, 2010.

[17] C. Zhang, H. You, Z. Lin, and Y. Hao, "Inverted organic photovoltaic cells with solution-processed zinc oxide as electron collecting layer," *Japanese Journal of Applied Physics*, vol. 50, no. 8, Article ID 082302, 2011.

[18] A. K. K. Kyaw, D. H. Wang, V. Gupta et al., "Efficient solution-processed small-molecule solar cells with inverted structure," *Advanced Materials*, vol. 25, no. 17, pp. 2397–2402, 2013.

[19] T. Kuwabara, H. Sugiyama, T. Yamaguchi, and K. Takahashi, "Inverted type bulk-heterojunction organic solar cell using electrodeposited titanium oxide thin films as electron collector electrode," *Thin Solid Films*, vol. 517, no. 13, pp. 3766–3769, 2009.

[20] G. Li, C. Chu, V. Shrotriya, J. Huang, and Y. Yang, "Efficient inverted polymer solar cells," *Applied Physics Letters*, vol. 88, no. 25, Article ID 253503, 2006.

[21] Y. Park, S. Noh, D. Lee, J. Kim, and C. Lee, "Study of the cesium carbonate (Cs_2CO_3) inter layer fabricated by solution process on P3HT:PCBM solar cells," *Molecular Crystals and Liquid Crystals*, vol. 538, no. 1, pp. 20–27, 2011.

[22] J. Zou, C.-Z. Li, C.-Y. Chang, H.-L. Yip, and A. K.-Y. Jen, "Interfacial engineering of ultrathin metal film transparent electrode for flexible organic photovoltaic cells," *Advanced Materials*, vol. 26, no. 22, pp. 3618–3623, 2014.

[23] Z. Lin, C. Jiang, C. Zhu, and J. Zhang, "Development of inverted organic solar cells with TiO_2 interface layer by using low-temperature atomic layer deposition," *ACS Applied Materials and Interfaces*, vol. 5, no. 3, pp. 713–718, 2013.

[24] H. Choi, J. S. Park, E. Jeong et al., "Combination of titanium oxide and a conjugated polyelectrolyte for high-performance inverted-type organic optoelectronic devices," *Advanced Materials*, vol. 23, no. 24, pp. 2759–2763, 2011.

[25] J. You, C.-C. Chen, L. Dou et al., "Metal oxide nanoparticles as an electron-transport layer in high-performance and stable inverted polymer solar cells," *Advanced Materials*, vol. 24, no. 38, pp. 5267–5272, 2012.

[26] Z. Lin, J. Chang, C. Jiang, J. Zhang, J. Wu, and C. Zhu, "Enhanced inverted organic solar cell performance by post-treatments of solution-processed ZnO buffer layers," *RSC Advances*, vol. 4, no. 13, pp. 6646–6651, 2014.

[27] J. Chang, Z. Lin, C. Zhu, C. Chi, J. Zhang, and J. Wu, "Solution-processed lif-doped ZnO films for high performance low temperature field effect transistors and inverted solar cells," *ACS Applied Materials and Interfaces*, vol. 5, no. 14, pp. 6687–6693, 2013.

[28] S. Y. Cho, Y. H. Kang, J.-Y. Jung et al., "Novel zinc oxide inks with zinc oxide nanoparticles for low-temperature, solution-processed thin-film transistors," *Chemistry of Materials*, vol. 24, no. 18, pp. 3517–3524, 2012.

[29] C. Zhang, J. Zhang, Y. Hao, Z. Lin, and C. Zhu, "A simple and efficient solar cell parameter extraction method from a single current-voltage curve," *Journal of Applied Physics*, vol. 110, no. 6, Article ID 064504, 2011.

[30] Y. H. Lin, H. Faber, K. Zhao et al., "High-performance ZnO transistors processed via an aqueous carbon-free metal oxide precursor route at temperatures between 80–180°C," *Advanced Materials*, vol. 25, no. 31, pp. 4340–4346, 2013.